RSC Advances

PAPER

View Article Online
View Journal | View Issue

Cite this: *RSC Adv.*, 2015, **5**, 45974

TiO_2-coated magnetite nanoparticle-supported sulfonic acid as a new, efficient, magnetically separable and reusable heterogeneous solid acid catalyst for multicomponent reactions†

Ali Amoozadeh,* Sanaz Golian and Salman Rahmani

Received 11th April 2015
Accepted 12th May 2015

DOI: 10.1039/c5ra06515a

www.rsc.org/advances

TiO_2-coated magnetite nanoparticle-supported sulfonic acid (nano-Fe_3O_4–TiO_2–SO_3H (n-FTSA)) is synthesized by immobilizing $-SO_3H$ groups on the surface of nano-Fe_3O_4–TiO_2. This catalyst can be isolated readily after completion of the reaction by an external magnetite field. The obtained results demonstrate the use of coated magnetite nanoparticles as an excellent new support for the facile recovery of sulfonic acid catalysts. The newly synthesized heterogeneous solid acid is characterized by X-ray diffraction (XRD), energy-dispersive X-ray spectroscopy (EDX), field emission scanning electron microscopy (FE-SEM), a vibrating sample magnetometer (VSM), FT-IR spectroscopy, thermal gravimetric analysis (TGA), Hammett acidity function and pH analysis. Significantly, the as-prepared n-FTSA exhibits a high catalytic activity for the synthesis of heterocyclic compounds such as 1,8-dioxo-decahydroacridine, 1,8-dioxo-octahydroxantene, hexahydroquinoline and polyhydroquinoline derivatives in multicomponent reactions. The magnetically separated n-FTSA can be magnetically separated and reused for several times without significant loss of activity. This confirms that the sulfonic acid groups have high stability. TiO_2-coated magnetite nanoparticle-supported sulfonic acid has advantages such as low cost and toxicity, ease of preparation, magnetic separation, high stability, reusability and operational simplicity.

1. Introduction

Very often the most exclusive components in chemical reactions are catalysts. Sulfuric, nitric, hydrochloric and phosphoric acid are the most important and commonly used homogeneous acid catalysts in organic reactions and industrial processes.[1] Among these, sulfuric acid is not a recyclable and environmentally benign material. Corrosive properties and inefficient separation from reaction mixtures leads to a huge waste of energy and production of large amounts of waste products. In spite of the aforementioned drawbacks, it is essential for chemical industries, too.[2] Recently, heterogenization of homogeneous catalysts by their immobilization on the surface of various solid supports has attracted great interest from the environmental and economic points of view.[2–16] In this regard, metal oxide nanoparticle supports are attractive due to their large surface area-to-volume.[17–21] As a result, nanoparticles have high catalyst loading capacity which leads to the improved performance. The active sites on their surfaces are easily available by reactants. Separation of the nanoparticles by conventional means is almost impossible. This problem is overcome by using magnetite nanoparticle as heterogeneous supports, which can be readily isolated from the reaction mixture in the presence of an external magnetite field.[22–37] An intrinsic disadvantage of bare magnetite nanoparticles is magnetite aggregation[38,39] that outside surface coating by metal oxides reduces lower this problem[40] and can be improved catalytic activity of the magnetite nanoparticles. Among the many metal oxides, titanium dioxide is attractive because of extra ordinary features and different applications in gas sensing,[41,42] catalysis,[43] photocatalysis[44–46] *etc.*

The synthesis of surface-modified magnetite nanoparticles is one of the major areas of current research in the field of catalysis.[47–53] The magnetite solid acid nanocatalysts have emerged as efficient and powerful in organic reactions because of high activity, easy separation, minimization of environmental waste and clean reaction products without contamination of active metals.[54] Based on the mentioned facts and in continuation of our last efforts and studies about synthesis of heterogeneous solid acid nanocatalysts[55,56] and their applications in organic reaction,[57–59] we decided to introduce a magnetically recoverable solid acid catalyst. For this purpose, we have designed and synthesized TiO_2-coated magnetite nanoparticles sulfonic acid (n-FTSA) and used it for some multicomponent reactions. As sulfonation with chlorosulfonic acid is a convenient, fast and efficient method for heterogenization of homogeneous

Department of Chemistry, Semnan University, Semnan, 35131-19111, Iran. E-mail: aamozadeh@semnan.ac.ir; Fax: +98 233 3354110; Tel: +98 233 3366177

† Electronic supplementary information (ESI) available: FE-SEM, VSM, TGA, reusability of the n-FTSA, ^1H NMR and ^{13}C NMR spectra. See DOI: 10.1039/c5ra06515a

catalysts[55,60–64] that has absorbed much attention after Zolfigol's report,[65] and as we have already successfully synthesized and reported nano-TiO_2–SO_3H (n-TSA) as an excellent heterogeneous nanocatalyst for different organic reactions,[55] we have decided to react the nano-Fe_3O_4–TiO_2 react with chlorosulfonic acid to produce nano-Fe_3O_4–TiO_2-supported sulfonic acid (nano-Fe_3O_4–TiO_2–SO_3H).

The new synthesized nano-Fe_3O_4–TiO_2–SO_3H catalyst has been successfully used for some multicomponent one-pot reactions to synthesis different heterocyclic compounds such as 1,8-dioxo-decahydroacridine, 1,8-dioxo-octahydroxantene, hexahydroquinoline and polyhydroquinoline derivatives. This novel nanocatalyst can be magnetically separated and recycled several runs without appreciable loss of its catalytic activity.

2. Results and discussion

The supported sulfonic acid analogue was prepared by the concise route outlined in Scheme 1.

Fe_3O_4/TiO_2 core–shell nanoparticles were prepared according to the reported procedure.[66]

2.1. Characterization of nano-Fe_3O_4/TiO_2–SO_3H

2.1.1. X-ray diffraction spectra. Fig. 1 shows the X-ray diffraction patterns of the synthesized nano-Fe_3O_4/TiO_2 core–shell and the acidic modified nano-Fe_3O_4/TiO_2–SO_3H (n-FTSA).

Fig. 1a shows the XRD pattern of nano-Fe_3O_4/TiO_2. The following signals at (220), (311), (400), (511) and (440) in Fig. 1a planes confirm that the main formed phase is a cubic Fe_3O_4, which conforms with the JCPD 79-0417 standard.

However, there are two other phases including SiO_2 with orthorhombic crystal structure (JCPDS: 44-1394) and TiO_2 with anatase crystal structure which conforms by (105), (211), (116), (220), (512) and (224) diffraction peaks (JCPDS: 89-4921). The crystal size of the nano-Fe_3O_4/TiO_2 powder was also determined from X-ray pattern using the Scherrer formula given as $t = 0.9\lambda/B_{1/2}\cos\theta$, that t is the average crystal size, λ the X-ray wavelength used (1.54 Å), $B_{1/2}$ the angular line width at half maximum intensity and θ the Bragg's angle. The average crystal size of the nano-Fe_3O_4–TiO_2 powder for $2\theta = 35.48°$ is calculated to be around 23 nm.

Fig. 1b shows the XRD pattern of nano-Fe_3O_4/TiO_2–SO_3H. It shows that with modifying nano-Fe_3O_4/TiO_2, the XRD pattern shows a higher noise/signal ratio indicating that the material has an acidic agent on their surface. The average crystal size of nano-Fe_3O_4/TiO_2–SO_3H for $2\theta = 35.61°$ is calculated to be around 22.75 nm. The interplanar spacing (d) was calculated by Bragg's equation using the peak at 35.48° and 35.61° for nano-Fe_3O_4/TiO_2 and nano-Fe_3O_4/TiO_2–SO_3H, respectively. $\Delta d = d(a) - d(b) = 0.253 - 0.238 = 0.015$ Å. So according to the data, there is a contraction in the unit cell.

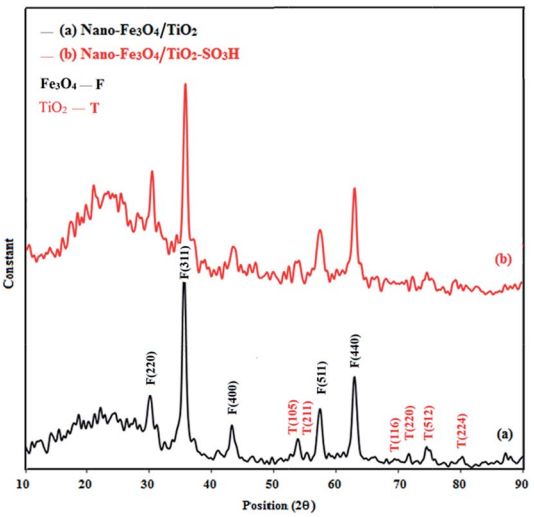

Fig. 1 X-ray diffraction pattern of (a) the nano-Fe_3O_4/TiO_2 and (b) nano-Fe_3O_4/TiO_2–SO_3H.

2.1.2. Energy-dispersive X-ray spectroscopy (EDX). The presence of Fe, O, Si and Ti atoms was observed in the EDX spectrum (Fig. 2).

2.1.3. Field emission scanning electron microscopy. According to the FE-SEM image of nano-Fe_3O_4/TiO_2, it was found that the morphology of the synthesized nano material has a sphere like structures. The size distribution and morphology of nanoparticles are almost homogeneous and diameter sizes obtained nanoparticles are about 50–60 nm.

The FE-SEM image of nano-Fe_3O_4/TiO_2–SO_3H shows that by modifying nano-Fe_3O_4/TiO_2 with SO_3H, the morphology of the obtained materials has been maintained particle structures. However the size distribution is nearly non-homogeneous.

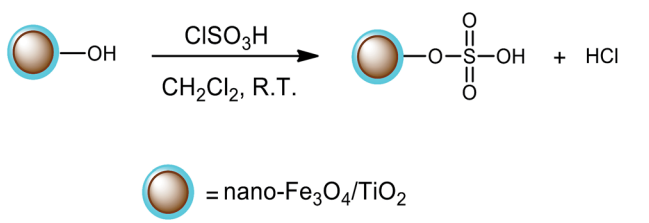

Scheme 1 Preparation of nano-Fe_3O_4/TiO_2-supported sulfonic acid.

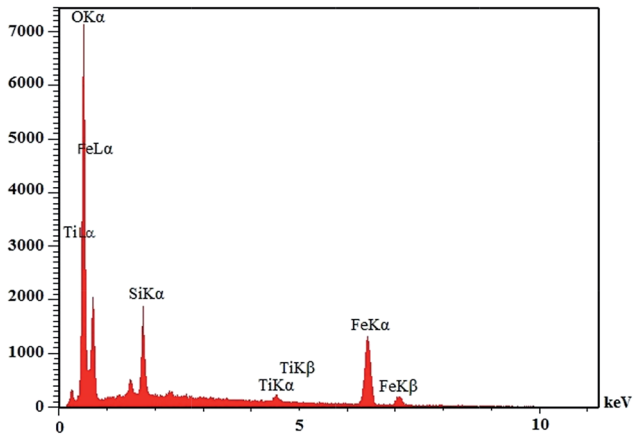

Fig. 2 EDX spectrum of nano-Fe_3O_4/TiO_2.

Since the size distribution of nano-Fe_3O_4/TiO_2 is not homogeneous, and there are small and large particles together in the structure, so there are two kinds of particles sizes. The diameter size for the small particles is about 40–60 nm and for the large particles is about 100–150 nm.

2.1.4. Vibrating sample magnetometer. The magnetite properties of the Fe_3O_4/TiO_2 nanoparticles and nano-Fe_3O_4/TiO_2–SO_3H have been measured by use of the vibrating sample magnetometer. The magnetization curves measured at room temperature showed that n-FTSA was super paramagnetic and had magnetization saturation value of 26.31 emu g^{-1}. The number is lower than that of TiO_2-coated magnetite nanoparticles (about 50 emu g^{-1}). The decrease in saturation magnetization after being coated is because of the immobilization of non-magnetite sulfonic acid groups on the surface of magnetite nanoparticles.

Nonetheless, the magnetization value is enough for common magnetite separation. As can be seen, n-FTSA was readily dispersible in reactive system and can be easily separated with a small magnet near the tube.

2.1.5. FT-IR spectra. The FT-IR spectra of nano-Fe_3O_4–TiO_2 and nano-Fe_3O_4–TiO_2–SO_3H are shown in Fig. 3. The O–H stretch and vibration of surface hydroxyl groups and physically adsorbed water were present as broad peaks at 3000–3600 cm^{-1} and a sharper peaks at 1628 cm^{-1} (a) and 1632 cm^{-1} (b), respectively. We assign the absorption band appears at 979 and 1080 cm^{-1} (a), 997 and 1092 cm^{-1} (b) to a combination of Ti–O–Si and Si–OH vibrations.[67–69]

As respects, the O=S=O asymmetric and symmetric stretching vibration and S–O stretching vibration of the sulfonic groups (–SO_3H) are appeared in the absorption range 1150–1250, 1010–1100 and 650–850 cm^{-1}, respectively.[70] Stretching vibrations of TiO_2 were observed in the absorption range of sulfonic groups so these bands have been hidden (Fig. 3b).

2.1.6. Thermo gravimetric analysis. According to the TGA curve of nano-Fe_3O_4/TiO_2 a mass loss (2 wt%) below 100 °C which corresponds to the loss of the physically adsorbed water. Also, there is a slight weight loss (1 wt%) between 100–440 °C and weight loss (5 wt%) between 440 and 800 °C, which possibly corresponds to the dehydroxylation of nano-Fe_3O_4/TiO_2.[71] The TGA curve of n-FTSA shows three regions corresponding to different mass lose ranges. The first region is below 100 °C that displayed a mass loss (3 wt%) that was attributable to the loss of trapped water from the catalyst. A mass loss of approximately 22.37% weight occurred between 100 and 540 °C that is related to the slow mass loss of SO_3H groups. Finally, a mass loss of approximately 15.46% weight occurred between 540 and 644 °C that is related to the sudden mass loss of SO_3H groups.[70,72,73] In addition, from the TGA, it is understood that n-FTSA has a great thermal stability (until 200 °C) confirming that it can be safely used in organic reactions at temperatures in the range of 80–180 °C.

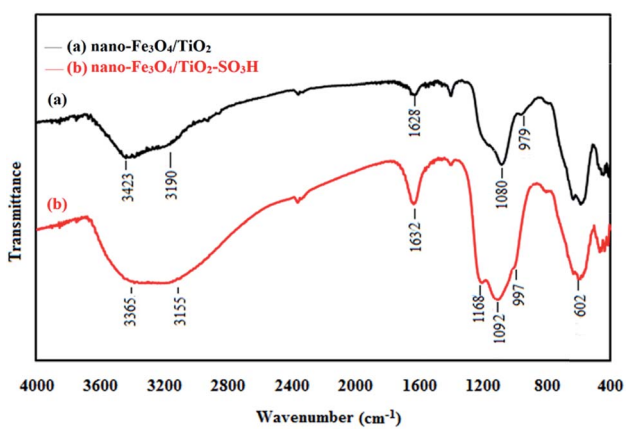

Fig. 3 The FT-IR spectra of (a) the nano-Fe_3O_4/TiO_2 and (b) nano-Fe_3O_4/TiO_2–SO_3H.

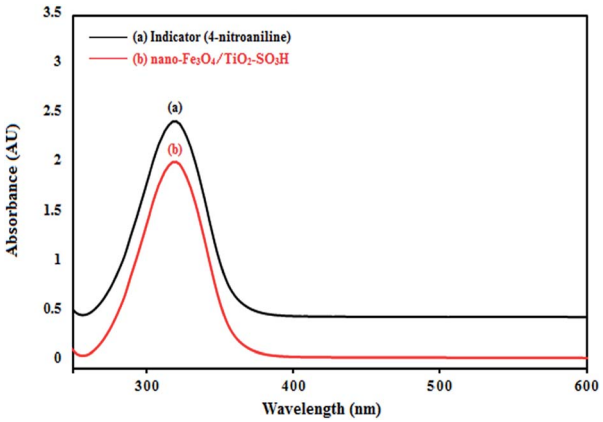

Fig. 4 Absorption spectra of (a) 4-nitroaniline (indicator) and (b) nano-Fe_3O_4/TiO_2–SO_3H (catalyst) in CCl_4.

2.1.7. Surface acidity studies. The Hammett acidity function (H_0) can effectively express the acidity strength of an acid in organic solvents.[74] It can be calculated using the following equation:

$$H_0 = pK(I)_{aq} + \log([I]_s/[IH^+]_s).$$

Here, 'I' represents the indicator base (mainly substituted nitroanilines) and $[I]_s$ and $[IH^+]_s$ are respectively the molar concentrations of the unprotonated and protonated forms of the indicator. The $pK(I)_{aq}$ values are already known (for example the $pK(I)_{aq}$ value of 4-nitroaniline is 0.99) and can be obtained from many references. According to the Lambert–Beer law, the value of $[I]_s/[IH^+]_s$ can be determined and calculated using the UV-visible spectrum. In the present experiment, 4-nitroaniline was chosen as the basic indicator and CCl_4 was chosen as the

Table 1 Calculation of Hammett acidity function (H_0) of n-FTSA[a]

Entry	Catalyst	A_{max}	$[I]_s$ (%)	$[IH^+]_s$ (%)	H_0
1	—	2.417	100	0	—
2	n-FTSA	1.987	82.64	17.36	1.75

[a] Condition for UV-visible spectrum measurement: solvent, CCl_4; indicator, 4-nitroaniline ($pK(I)_{aq}$ = 0.99), 1.44 × 10^{-4} mol L^{-1}; catalyst, n-FTSA (10 mg), 25 °C.

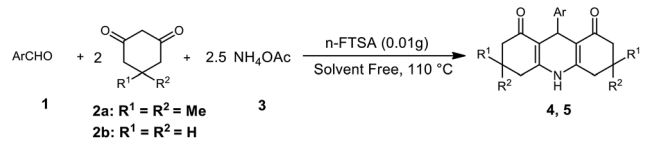

Scheme 2 Synthesis of 1,8-dioxodecahydroacridine derivatives catalyzed by n-FTSA.

solvent because of its aprotic nature. The maximal absorbance of the unprotonated form of 4-nitroaniline was observed at 330 nm in CCl_4. As Fig. 4 shows, the absorbance of the unprotonated form of the indicator in n-FTSA was weak as compared to the sample of the indicator in CCl_4, which indicated that the indicator was partially in the form of $[IH^+]$.

The obtained results are listed in Table 1, which shows the acidity strength of nano-Fe_3O_4–TiO_2–SO_3H. These results of the Hammett acidity function (H_0) also confirm the synthesis of new catalyst with a good density of acid sites (–SO_3H groups) on the surface of n-FTSA (Table 1).

The mmol of H^+ per gram of catalyst (5 mmol g^{-1} of n-FTSA) was determined by the titration of 0.1 g of sample with a standard solution of NaOH (0.1 N). For this purpose, the surface acidic protons of n-FTSA (100 mg) were ion-exchanged with a saturated solution of NaCl (10 mL) by sonication. This process was repeated twice more, yielding 30 mL of proton-exchanged brine solution. Therefore, to determine the loading of acid sites on the synthesized catalyst, the obtained solution was titrated by NaOH (0.1 M) solution in presence of phenol red indicator solution or pH meter.

2.2. Investigating of nano-Fe_3O_4–TiO_2–SO_3H in one-pot multicomponent reactions

In continuation of our studies on the development of solid acids as efficient, inexpensive and also environmentally benign methodologies for organic reactions,[57–59] we have recently reported nano-titania-supported sulfonic acid,[55] nano-WO_3-supported sulfonic acid[56] as novel and heterogeneous nanocatalyst. Also chromium trioxide-supported sulfonic acid was studied where the results were also very satisfactory.

Table 2 Optimization of catalyst amount for the synthesis of tetramethyl-9-phenyl-hexahydroacridine-dione[a]

Entry	Catalyst (g)	Yield[b] [%]
1	—	8
2	Bulk-TiO_2	24
3	Nano-TiO_2	43
4	Bulk-Fe_2O_3	28
5	Nano-Fe_2O_3	49
6	Nano-Fe_3O_4	50
7	Nano-Fe_3O_4–TiO_2	60
8	n-FTSA (0.015)	95
9	n-FTSA (0.01)	95
10	n-FTSA (0.005)	75

[a] Reaction conditions: benzaldehyde (1 mmol), dimedone (2 mmol), NH_4OAc (2.5 mmol), solvent free, 110 °C. [b] Refers to isolated yield.

Table 3 Effect of temperature on the n-FTSA catalyzed synthesis of tetramethyl-9-phenyl-hexahydroacridine-dione[a]

Entry	Temperature [°C]	Yield[b] [%]
1	80	70
2	90	70
3	100	85
4	110	95
5	120	80

[a] Reaction conditions: benzaldehyde (1 mmol), dimedone (2 mmol), NH_4OAc (2.5 mmol), n-FTSA (0.01 g), solvent free. [b] Refers to isolated yield.

On the basis of the information obtained from the above mentioned studies, in this context, we synthesized nano-Fe_3O_4/TiO_2-supported sulfonic acid (nano-Fe_3O_4/TiO_2–SO_3H) with highly density of sulfonic acid groups (–SO_3H) and introduced as a novel, highly efficient and strong, stable, magnetically separable, reusable and inexpensive heterogeneous solid acid. The catalytic activity of new nanocatalyst was examined in multicomponent reactions for the synthesis of heterocyclic compounds such as 1,8-dioxo-decahydroacridine, 1,8-dioxo-octahydroxanthene, polyhydroquinoline and hexahydroquinoline derivatives. The structures of the some final products were well characterized by using spectral (IR, ^{1}H NMR, ^{13}C NMR) data.

2.2.1. Synthesis of 1,8-dioxo-decahydroacridine derivatives. In the first glance, in order to initially optimize the reaction conditions and identity of the best amount of catalyst, benzaldehyde **1**, cyclic-diketone **2a** and ammonium acetate **3** were stirred under solvent free conditions in 110 °C (Scheme 2).

By screening different amounts of the n-FTSA and comparing with other sources of iron and titanium, we found out that the product **4a** could be obtained in yields ranging from

Table 4 n-FTSA catalyzed synthesis of 1,8-dioxo-decahydroacridines[a]

R^1=R^2	Ar	Product	Time (min)	Yield[b] [%]
Me	Ph	**4a**	50	95
Me	*p*-Cl–C_6H_4	**4b**	40	95
Me	*o*-Cl–C_6H_4	**4c**	45	94
Me	*p*-O_2N–C_6H_4	**4d**	25	96
Me	*m*-O_2N–C_6H_4	**4e**	25	95
Me	*p*-$(CH_3)_2N$–C_6H_4	**4f**	50	90
Me	*p*-HO–C_6H_4	**4g**	55	90
Me	*p*-H_3C–C_6H_4	**4h**	60	92
Me	*p*-H_3CO–C_6H_4	**4i**	60	93
H	Ph	**5a**	50	90
H	*m*-O_2N–C_6H_4	**5b**	40	94
H	*p*-Cl–C_6H_4	**5c**	45	94
H	*p*-Br–C_6H_4	**5d**	45	94
H	*p*-H_3C–C_6H_4	**5e**	60	92
H	*p*-HO–C_6H_4	**5f**	55	90

[a] Reaction conditions: aromatic aldehyde (1 mmol), cyclic di-ketone (2 mmol), NH_4OAc (2.5 mmol), n-FTSA (0.01 g) under solvent free conditions at 110 °C. [b] Yields refer to isolated products.

Table 5 Reuse of n-FTSA in the synthesis of tetramethyl-9-phenyl-hexahydroacridine-dione[a]

Run	1	2	3	4	5
Yield[b] [%]	95	95	94	93	93

[a] Benzaldehyde **1** (1 mmol), dimedone **2a** (2 mmol), NH_4OAc **3** (2.5 mmol), solvent free conditions at 110 °C. [b] Isolated yields.

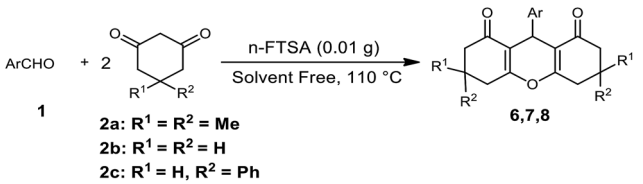

Scheme 3 Synthesis of 1,8-dioxo-octahydroxanthene derivatives catalyzed by n-FTSA.

60 to 95%. The best yield was obtained by using 0.01 g of n-FTSA (Table 2, entry 9) and is a more suitable option than nano-Fe_3O_4–TiO_2 (Table 2, entry 7). Also, the obtained results of other catalysts showed low yields of product **4a**. The greater catalytic activity of n-FTSA was most likely related to the SO_3H groups of the catalyst, which could provide efficient acidic sites.

In the next step, to study the effect of temperature was investigated. The results showed that the best temperature was 110 °C (Table 3, entry 4) and the obtained yield remained unchanged by increasing the temperature to 120 °C.

After optimizing the conditions (n-FTSA (0.01 g) at 110 °C under solvent free conditions), the scope of method and catalytic activity of new nanocatalyst was successfully studied by using various aromatic aldehydes (including aldehydes with electron-releasing substituents, electron-withdrawing substituents and halogens on the aromatic ring) and cyclic 1,3-di-ketone compounds. The obtained results are summarized in Table 4.

Table 6 n-FTSA catalyzed synthesis of xanthenes[a]

R^1	R^2	Ar	Product	Time (min)	Yield[b] [%]
Me	Me	Ph	**6a**	50	90
Me	Me	*p*-Cl–C_6H_4	**6b**	40	89
Me	Me	*p*-O_2N–C_6H_4	**6c**	42	91
Me	Me	*m*-O_2N–C_6H_4	**6d**	45	88
Me	Me	*p*-HO–C_6H_4	**6e**	57	82
Me	Me	*p*-H_3C–C_6H_4	**6f**	55	85
Me	Me	*p*-H_3CO–C_6H_4	**6g**	55	86
H	H	Ph	**7a**	52	88
H	H	*p*-O_2N–C_6H_4	**7b**	45	89
H	H	*p*-Br–C_6H_4	**7c**	42	86
H	H	*p*-H_3C–C_6H_4	**7d**	52	84
H	Ph	Ph	**8a**	52	86
H	Ph	*p*-Cl–C_6H_4	**8b**	55	85
H	ph	*p*-H_3C–C_6H_4	**8c**	55	85
H	Ph	*p*-H_3CO–C_6H_4	**8d**	47	87

[a] Reaction conditions: aromatic aldehyde (1 mmol), cyclic di-ketone (2 mmol), n-FTSA (0.01 g) under solvent free conditions at 110 °C. [b] Yields refer to isolated products.

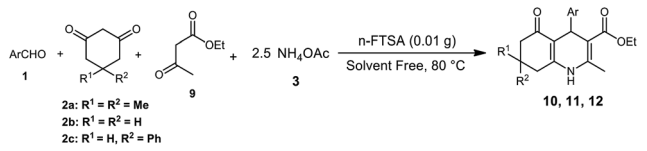

Scheme 4 Synthesis of polyhydroquinoline derivatives catalyzed by n-FTSA.

Because of ferromagnetic features, the separation and reuse of n-FTSA is very facile. In this regard, the catalyst was washed with hot ethanol and acetone twice and then was dried in the open air. The recycled catalyst could be reused for at least five times with no appreciable decrease in yield of product **4a** (Table 5).

2.2.2. Synthesis of 1,8-dioxo-octahydroxanthene derivatives. The prepared n-FTSA has been tested for the synthesis of 1,8-dioxo-octahydroxanthene derivatives under optimal conditions by condensation between aromatic aldehydes **1** (1 mmol) and cyclic di-ketones **2** (2 mmol) (Scheme 3). The results are recorded in Table 6.

2.2.3. Synthesis of polyhydoquinoline derivatives. The efficiency of obtained n-FTSA has been tested by the synthesis of polyhydroquinoline derivatives under optimal conditions by condensation between benzaldehyde **1** (1 mmol), ethyl-acetoacetate **9** (1 mmol), cyclic di-ketones **2a–c** (1 mmol) and ammonium acetate **3** (2.5 mmol) (Scheme 4). The results are summarized in Table 7.

2.2.4. Synthesis of hexahydroquinoline derivatives. The catalytic activity of n-FTSA has been examined for the synthesis of hexahydroquinoline derivatives under optimal conditions with condensation benzaldehyde **1** (1 mmol), cyclic di-ketones **2**

Table 7 n-FTSA catalyzed synthesis of polyhydroquinolines[a]

R^1	R^2	Ar	Product	Time (min)	Yield[b] [%]
Me	Me	Ph	**10a**	10	97
Me	Me	*p*-O_2N–C_6H_4	**10b**	5	97
Me	Me	*m*-O_2N–C_6H_4	**10c**	9	97
Me	Me	*p*-Cl–C_6H_4	**10d**	5	95
Me	Me	*o*-Cl–C_6H_4	**10e**	7	95
Me	Me	*p*-HO–C_6H_4	**10f**	15	96
Me	Me	*p*-H_3C–C_6H_4	**10g**	15	97
Me	Me	*p*-$(CH_3)_2N$–C_6H_4	**10f**	20	92
H	H	Ph	**11a**	13	96
H	H	*p*-O_2N–C_6H_4	**11b**	54	94
H	H	*p*-Cl–C_6H_4	**11c**	5	91
H	H	*p*-H_3C–C_6H_4	**11d**	17	97
H	H	*p*-HO–C_6H_4	**11e**	15	89
H	Ph	Ph	**12a**	15	95
H	Ph	*p*-Cl–C_6H_4	**12b**	5	96
H	Ph	*p*-H_3CO–C_6H_4	**12c**	17	97

[a] Reaction conditions: aromatic aldehyde (1 mmol), cyclic di-ketone (1 mmol), NH_4OAc (2.5 mmol), ethylacetoacetate (1 mmol), n-FTSA (0.01 g) under solvent free conditions at 80 °C. [b] Yields refer to isolated products.

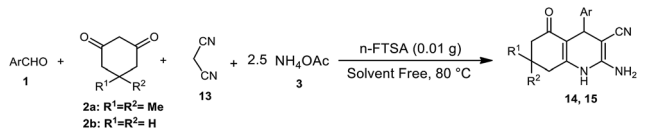

Scheme 5 Synthesis of hexahydroquinoline derivatives catalyzed by n-FTSA.

Table 8 n-FTSA catalyzed synthesis of hexahydroquinolines[a]

R^1=R^2	Ar	Product	Time (min)	Yield[b] [%]
Me	Ph	**14a**	10	92
Me	*p*-Cl–C_6H_4	**14b**	5	95
Me	*o*-Cl–C_6H_4	**14c**	5	91
Me	*p*-Br–C_6H_4	**14d**	7	95
Me	*m*-O_2N–C_6H_4	**14e**	7	94
Me	*p*-H_3C–C_6H_4	**14f**	15	90
Me	*p*-$(CH_3)_2N$–C_6H_4	**14g**	15	89
Me	*p*-H_3CO–C_6H_4	**14h**	15	90
H	Ph	**15a**	12	92
H	*p*-Cl–C_6H_4	**15b**	11	93
H	*o*-Cl–C_6H_4	**15c**	12	92
H	*p*-O_2N–C_6H_4	**15d**	7	94
H	*m*-O_2N–C_6H_4	**15e**	9	91
H	*p*-H_3C–C_6H_4	**15f**	13	89
H	*p*-H_3CO–C_6H_4	**15g**	14	88

[a] Reaction conditions: aromatic aldehyde (1 mmol), cyclic di-ketone (1 mmol), NH_4OAc (2.5 mmol), malononitrile (1 mmol) n-FTSA (0.01 g) under solvent free conditions at 80 °C. [b] Yields refer to isolated products.

(1 mmol), malononitrile **13** (1 mmol) and ammonium acetate **3** (2.5 mmol) (Scheme 5). The results are listed in Table 8.

2.3. Reusability of the n-FTSA

For practical applications of this heterogeneous solid acid catalyst, the level of reusability was also tested. The recycled catalyst could be reused for at least five times with no appreciable decrease in yield. It signified that the nature of the catalyst remains intact after each run and $-SO_3H$ moiety was tightly anchored with nano-Fe_3O_4/TiO_2, most probably through a covalent linkage.

3. Experimental section

3.1. General remarks

Chemicals were purchased from the Merck chemical companies. Nano-Fe_3O_4/TiO_2 was prepared with the reported method.[66] Fourier transform infrared spectroscopy (FTIR) was recorded on a Shimadzu 8400s spectrometer using KBr pressed powder discs. ^1H NMR and ^{13}C NMR spectra which were recorded on Bruker Advance Spectrometer 400 & 500 MHz using $CDCl_3$-d and DMSO-d_6 as solvent. The chemical shifts are expressed in parts per million (ppm) and tetramethylsilane (TMS) was used as an internal reference. Wide-angle X-ray diffraction (XRD) spectrum for the n-FTSA powder sample was obtained using a Siemens D5000 (Siemens AG, Munich, Germany) X-ray diffractometer using Cu-Kα radiation of wavelength 1.54 Å. The EDX characterization of the catalyst was performed using a Mira 3-XMU scanning electron microscope equipped with an energy dispersive X-ray spectrometer operating. A particle size study of n-FTSA sample was carried out using Philips XL30 field emission scanning electron microscope (FE-SEM) (Royal Philips Electronics, Amsterdam, The Netherlands) instrument operating at 10 kV. The sample was mounted on a double-sided adhesive carbon disk and sputter-coated with a thin layer of gold to prevent sample charging problems. Thermo gravimetric analyses (TGA) were conducted on a Du Pont 2000 thermal analysis apparatus under air atmosphere at a heating rate of 5 °C min^{-1}. The magnetite measurement was carried out in a vibrating sample magnetometer (VSM) (4 inch, Daghigh Meghnatis Kashan Co., Kashan, Iran) at room temperature.

3.2. Preparation of iron oxide magnetite nanoparticles

Both $FeCl_2$ (2 g) and $FeCl_3$ (5.4 g) were dissolved in aqueous hydrochloric acid (2 M, 25 mL), and the air in the mixture was eliminated using a pump. The mixture was stirred for 10 min under nitrogen followed by the addition of aqueous ammonia (28%, 40 mL) with stirring. After 1 h, the generated iron oxide nanoparticles were rinsed with deionized water two or three times.

3.3. Preparation of titania-coated iron oxide (nano-Fe_3O_4/TiO_2) magnetite nanoparticles

The nanoparticles generated above (0.2 g) were rinsed with ethanol three times and then resuspended in ethanol (40 mL) under sonication for 1 h. Aqueous ammonia (4.5 mL), deionized water (3.75 mL), and TEOS (0.1 mL) were added in sequence to the suspension. The mixture was sonicated for 1 h followed by vortex mixing for another 8 h. The silica modified nanoparticles were isolated by magnetite separation and were rinsed with ethanol two or three times. The nanoparticles were resuspended in ethanol (40 mL) followed by refluxing at 60 °C for 12 h. After rinsing with deionized water, the generated nanoparticles were resuspended in deionized water (40 mL) and the suspension was acidified with nitric acid (0.5 M, 0.22 mL)/deionized water (124.78 mL) solution. The suspension was heated at 60 °C, and a solution containing titanium isopropoxide (15 μL) and 2-propanol (11.985 mL) was slowly added to the mixture under stirring for 6 h. TEOS, titanium isopropoxide, and DMF are toxic. They should be handled with care by preparing the reagents in a hood and wearing gloves if necessary. The generated nano-Fe_3O_4/TiO_2 magnetite nanoparticles were rinsed with deionized water twice. Direct contact of the nanoparticles with the hands should be avoided as the nanoparticles have photocatalytic activity.

3.4. Preparation of the nano-Fe_3O_4/TiO_2–SO_3H (n-FTSA)

A suction flask equipped with a constant-pressure dropping funnel and a gas inlet tube for conducting HCl gas over an adsorbing solution (*i.e.*, water) was used, charged with the nano-Fe_3O_4/TiO_2 (0.2 g) in dry CH_2Cl_2 (10 mL). Then chlorosulfonic acid (0.05 mL) was added drop wisely over a period of

30 min at room temperature. (**Caution**: a highly corrosive and water absorbant. Be careful when using this liquid. Protective gloves, protective clothing and eye and face protection equipment are needed.)

HCl gas immediately evolved from the reaction vessel. Stirring was continued until HCl evolution was seized. After the addition was completed, the mixture was shaken for 30 min. A powder of nano-Fe_3O_4/TiO_2 supported sulfonic acid was obtained. Then, the CH_2Cl_2 was removed under reduced pressure and the solid powder was washed with ethanol (10 mL) and dried at 70 °C.

The prepared n-FTSA stored in vacuum desiccator over anhydrous silica gel, then, was dried in 120 °C for 6 hours.

3.5. General procedure for the synthesis of 1,8-dioxo-decahydroacridine derivatives

In a typical experiment, a mixture of different aromatic aldehydes **1** (1 mmol), cyclic di-ketones **2** (2 mmol) and ammonium acetate **3** (2.5 mmol) as the nitrogen source and n-FTSA (0.01 g) were added in a glass reactor under solvent free conditions at 110 °C were stirred for an appropriate time. The progress of the reaction was monitored by TLC, after completion of the reaction, hot ethanol was added to the reaction flask. The catalyst was isolated by external magnetite field. Solution was cooled to room temperature and crude product was recrystallized from ethanol to yield pure acridine derivatives.

3.6. General procedure for the synthesis of 1,8-dioxo-octahydroxanthene derivatives

In a typical experiment, a mixture of different aromatic aldehydes **1** (1 mmol), cyclic di-ketones **2** (2 mmol) and n-FTSA (0.01 g) were added in a 25 mL round bottomed flask under solvent free conditions at 110 °C were stirred for an appropriate time. The progress of the reaction was monitored by TLC, after completion of the reaction, hot ethanol was added to the reaction flask. The catalyst was isolated by external magnetite field and remained. Solution was cooled to room temperature and crude product was recrystallized from ethanol to yield pure 1,8-dioxo-octahydroxanthene derivatives.

3.7. General procedure for the synthesis of polyhydroquinoline derivatives

In a typical experiment, a mixture of different aromatic aldehydes **1** (1 mmol), cyclic di-ketones **2** (1 mmol), ethylacetoacetate **9** (1 mmol), ammonium acetate **3** (2.5 mmol) as the nitrogen source and n-FTSA (0.01 g) were added in a glass reactor under solvent free conditions at 80 °C were stirred for an appropriate time. The progress of the reaction was monitored by TLC, after completion of the reaction, hot ethanol was added to the reaction flask. The catalyst was isolated by external magnetite field. Solution was cooled to room temperature and crude product was recrystallized from ethanol to yield pure polyhydroquinoline derivatives.

3.8. General procedure for the synthesis of hexahydroquinoline derivatives

In a typical experiment, a mixture of different aromatic aldehydes **1** (1 mmol), cyclic di-ketones **2** (1 mmol), malononitrile **13** (1 mmol), ammonium acetate **3** (2.5 mmol) as the nitrogen source and n-FTSA (0.01 g) were added in a glass reactor under solvent free conditions at 80 °C were stirred for an appropriate time. The progress of the reaction was monitored by TLC, after completion of the reaction, hot ethanol was added to the reaction flask. The catalyst was isolated by external magnetite field and remained. Solution was cooled to room temperature and crude product was recrystallized from ethanol to yield pure hexahydroquinoline derivatives.

3.9. General procedure for recycling of n-FTSA

Recyclability of nano-Fe_3O_4–TiO_2-supported sulfonic acid (0.01 g) was tested for the synthesis of tetramethyl-9-phenyl-hexahydroacridine-dione between benzaldehyde **1** (1 mmol), dimedone **2a** (2 mmol), NH_4OAc **3** (2.5 mmol), under solvent free conditions for 50 min at 110 °C. After completion of the reaction, the heterogeneous catalyst was easily separated from the production mixture by external magnetite field, washed with ethanol (2 × 15 mL), acetone (2 × 10 mL) to remove the organic compounds and dried in oven to be used in the next cycles. In every run, the yield of product was performed in constant time. This process was repeated five more times, affording the desired product in good yields, with undiminishing efficiency.

4. Conclusion

In summary, for the first time, we have reported nano-Fe_3O_4–TiO_2-supported sulfonic acid (nano-Fe_3O_4–TiO_2–SO_3H) as a high-performance heterogeneous solid acid nanocatalyst for the synthesis of 1,8-dioxo-decahydroacridine, 1,8-dioxo-octahydroxantene, polyhydroquinoline and hexahydroquinoline derivatives. High catalytic activity, reusability, easy magnetically separability and environmental acceptability as compared to liquid acid catalyst make it a powerful solid acid catalyst for various organic reactions.

Acknowledgements

We gratefully acknowledge the Faculty of chemistry of Semnan University for supporting this work.

References

1 M. B. Smith and J. March, *March's advanced organic chemistry: reactions, mechanisms, and structure*, John Wiley & Sons, 2007.
2 A. Corma and H. Garcia, *Adv. Synth. Catal.*, 2006, **348**, 1391–1412.
3 P. T. Anastas and M. M. Kirchhoff, *Acc. Chem. Res.*, 2002, **35**, 686–694.
4 P. T. Anastas and J. B. Zimmerman, *Environ. Sci. Technol.*, 2003, **37**, 94A–101A.

5 J. H. Clark, *Acc. Chem. Res.*, 2002, **35**, 791–797.
6 S. M. Haile, D. A. Boysen, C. R. Chisholm and R. B. Merle, *Nature*, 2001, **410**, 910–913.
7 B. Horton, *Nature*, 1999, **400**, 797–799.
8 M. Misono, *C. R. Acad. Sci., Ser. IIc: Chim.*, 2000, **3**, 471–475.
9 T. Okuhara, *Chem. Rev.*, 2002, **102**, 3641–3666.
10 K. Smith, G. A. El-Hiti, A. J. Jayne and M. Butters, *Org. Biomol. Chem.*, 2003, **1**, 1560–1564.
11 P. W. Davies, *Annu. Rep. - R. Soc. Chem., Sect. B: Org. Chem.*, 2009, **105**, 93–112.
12 J. A. Gladysz, *Chem. Rev.*, 2002, **102**, 3215–3216.
13 A. Corma and H. Garcia, *Catal. Today*, 1997, **38**, 257–308.
14 C. S. Gill, B. A. Price and C. W. Jones, *J. Catal.*, 2007, **251**, 145–152.
15 J. A. Melero, G. D. Stucky, R. van Grieken and G. Morales, *J. Mater. Chem.*, 2002, **12**, 1664–1670.
16 J. A. Melero, R. van Grieken and G. Morales, *Chem. Rev.*, 2006, **106**, 3790–3812.
17 J. H. Fendler, Nanoparticles and Nanostructured Films, *Preparation, Characterization, and Applications*, John Wiley & Sons, 2008.
18 G. Schmid, *Nanoscale Mater. Chem.*, 2001, 15–59.
19 A. M. Molenbroek, S. Helveg, H. Topsøe and B. S. Clausen, *Top. Catal.*, 2009, **52**, 1303–1311.
20 R. Rodríguez, R. Nava, T. Halachev and V. M. Castano, *Macromol. Rapid Commun.*, 2004, **25**, 643–646.
21 N. Koukabi, E. Kolvari, M. A. Zolfigol, A. Khazaei, B. S. Shaghasemi and B. Fasahati, *Adv. Synth. Catal.*, 2012, **354**, 2001–2008.
22 S. Sá, M. B. Gawande, A. Velhinho, J. P. Veiga, N. Bundaleski, J. Trigueiro, A. Tolstogouzov, O. M. Teodoro, R. Zboril and R. S. Varma, *Green Chem.*, 2014, **16**, 3494–3500.
23 M. B. Gawande, R. Luque and R. Zboril, *ChemCatChem*, 2014, **6**, 3312–3313.
24 M. B. Gawande, Y. Monga, R. Zboril and R. Sharma, *Coord. Chem. Rev.*, 2015, **288**, 118–143.
25 I. Hsing, Y. Xu and W. Zhao, *Electroanalysis*, 2007, **19**, 755–768.
26 S. Shylesh, L. Wang, S. Demeshko and W. R. Thiel, *ChemCatChem*, 2010, **2**, 1543–1547.
27 Z. Gao, J. Zhou, F. Cui, Y. Zhu, Z. Hua and J. Shi, *Dalton Trans.*, 2010, 11132–11135.
28 C. W. Lim and I. S. Lee, *Nano Today*, 2010, **5**, 412–434.
29 S. Luo, X. Zheng and J.-P. Cheng, *Chem. Commun.*, 2008, 5719–5721.
30 S. Luo, X. Zheng, H. Xu, X. Mi, L. Zhang and J. P. Cheng, *Adv. Synth. Catal.*, 2007, **349**, 2431–2434.
31 K. V. Ranganath, J. Kloesges, A. H. Schäfer and F. Glorius, *Angew. Chem., Int. Ed.*, 2010, **49**, 7786–7789.
32 A. Schätz, O. Reiser and W. J. Stark, *Chem.–Eur. J.*, 2010, **16**, 8950–8967.
33 B. G. Wang, B. C. Ma, Q. Wang and W. Wang, *Adv. Synth. Catal.*, 2010, **352**, 2923–2928.
34 Z. Xu, H. Li, G. Cao, Z. Cao, Q. Zhang, K. Li, X. Hou, W. Li and W. Cao, *J. Mater. Chem.*, 2010, **20**, 8230–8232.
35 X. Zheng, S. Luo, L. Zhang and J.-P. Cheng, *Green Chem.*, 2009, **11**, 455–458.
36 Y. Zhu, L. P. Stubbs, F. Ho, R. Liu, C. P. Ship, J. A. Maguire and N. S. Hosmane, *ChemCatChem*, 2010, **2**, 365–374.
37 S. L. Brock and K. Senevirathne, *J. Solid State Chem.*, 2008, **181**, 1552–1559.
38 A. Hu, G. T. Yee and W. Lin, *J. Am. Chem. Soc.*, 2005, **127**, 12486–12487.
39 O. Gleeson, R. Tekoriute, Y. K. Gun'ko and S. J. Connon, *Chem.–Eur. J.*, 2009, **15**, 5669–5673.
40 A. H. Lu, E. e. L. Salabas and F. Schüth, *Angew. Chem., Int. Ed.*, 2007, **46**, 1222–1244.
41 E. Traversa, M. L. Di Vona, S. Licoccia, M. Sacerdoti, M. C. Carotta, L. Crema and G. Martinelli, *J. Sol-Gel Sci. Technol.*, 2001, **22**, 167–179.
42 V. Guidi, M. Carotta, M. Ferroni, G. Martinelli, L. Paglialonga, E. Comini and G. Sberveglieri, *Sens. Actuators, B*, 1999, **57**, 197–200.
43 W. J. Stark, S. E. Pratsinis and A. Baiker, *CHIMIA Int. J. Chem.*, 2002, **56**, 485–489.
44 Z. Zhang, C.-C. Wang, R. Zakaria and J. Y. Ying, *J. Phys. Chem. B*, 1998, **102**, 10871–10878.
45 A. Fuerte, M. D. Hernandez-Alonso, A. J. Maira, A. Martinez-Arias, M. Fernandez-Garcia, J. C. Conesa and J. Soria, *Chem. Commun.*, 2001, 2718–2719, DOI: 10.1039/B107314A.
46 M. Andersson, L. Österlund, S. Ljungstroem and A. Palmqvist, *J. Phys. Chem. B*, 2002, **106**, 10674–10679.
47 S. Mandal, D. Roy, R. V. Chaudhari and M. Sastry, *Chem. Mater.*, 2004, **16**, 3714–3724.
48 R. Tatumi, T. Akita and H. Fujihara, *Chem. Commun.*, 2006, 3349–3351.
49 M. A. White, J. A. Johnson, J. T. Koberstein and N. J. Turro, *J. Am. Chem. Soc.*, 2006, **128**, 11356–11357.
50 Y. Niu, L. K. Yeung and R. M. Crooks, *J. Am. Chem. Soc.*, 2001, **123**, 6840–6846.
51 L. N. Lewis, *Chem. Rev.*, 1993, **93**, 2693–2730.
52 R. S. Underhill and G. Liu, *Chem. Mater.*, 2000, **12**, 3633–3641.
53 M. Tamura and H. Fujihara, *J. Am. Chem. Soc.*, 2003, **125**, 15742–15743.
54 A. Wight and M. Davis, *Chem. Rev.*, 2002, **102**, 3589–3614.
55 S. Rahmani, A. Amoozadeh and E. Kolvari, *Catal. Commun.*, 2014, **56**, 184–188.
56 A. Amoozadeh and S. Rahmani, *J. Mol. Catal. A: Chem.*, 2015, **396**, 96–107.
57 A. Amoozadeh, R. A. Azadeh, S. Rahmani, M. Salehi, M. Kubicki and G. Dutkiewicz, *Phosphorus, Sulfur, and Silicon*, 2015.
58 A. Amoozadeh, E. Tabrizian and S. Rahmani, *C. R. Chim.*, 2015.
59 E. Kolvari, A. Amoozadeh, N. Koukabi, S. Otokesh and M. Isari, *Tetrahedron Lett.*, 2014, **55**, 3648–3651.
60 A. Shaabani, A. Rahmati and Z. Badri, *Catal. Commun.*, 2008, **9**, 13–16.
61 M. B. Gawande, A. K. Rathi, I. D. Nogueira, R. S. Varma and P. S. Branco, *Green Chem.*, 2013, **15**, 1895–1899.
62 M. B Gawande, R. Hosseinpour and R. Luque, *Curr. Org. Synth.*, 2014, **11**, 526–544.

63 K. Debnath, K. Singha and A. Pramanik, *RSC Adv.*, 2015, **5**, 31866–31877.
64 X.-N. Zhao, G.-F. Hu, M. Tang, T.-T. Shi, X.-L. Guo, T.-T. Li and Z.-H. Zhang, *RSC Adv.*, 2014, **4**, 51089–51097.
65 M. A. Zolfigol, *Tetrahedron*, 2001, **57**, 9509–9511.
66 W. J. Chen, P. J. Tsai and Y. C. Chen, *Small*, 2008, **4**, 485–491.
67 M. D. Alba, Z. Luan and J. Klinowski, *J. Phys. Chem.*, 1996, **100**, 2178–2182.
68 A. Lopez, M. Tuilier, J. Guth, L. Delmotte and J. Popa, *J. Solid State Chem.*, 1993, **102**, 480–491.
69 Y. Kotani, A. Matsuda, T. Kogure, M. Tatsumisago and T. Minami, *Chem. Mater.*, 2001, **13**, 2144–2149.
70 H. R. Shaterian, M. Ghashang and M. Feyzi, *Appl. Catal., A*, 2008, **345**, 128–133.
71 S. V. Atghia and S. S. Beigbaghlou, *J. Nanostruct. Chem.*, 2013, **3**, 1–8.
72 F. Nemati, M. M. Heravi and R. S. Rad, *Chin. J. Catal.*, 2012, **33**, 1825–1831.
73 M. Zolfigol, V. Khakyzadeh, A. Moosavi-Zare, G. Chehardoli, F. Derakhshan-Panah, A. Zare and O. Khaledian, *Sci. Iran.*, 2012, **19**, 1584–1590.
74 H. Xing, T. Wang, Z. Zhou and Y. Dai, *J. Mol. Catal. A: Chem.*, 2007, **264**, 53–59.